Solution Behavior of the Zwitterionic Surfactant Octadecyldimethylbetaine

Daniel Harrison,[†] Rita Szule,[‡] and Michael R. Fisch*

Department of Physics, John Carroll University, University Heights, Ohio 44118

Received: April 22, 1998; In Final Form: June 23, 1998

A light scattering, viscosity, surface tension, and cryo-TEM study was performed on aqueous solutions of octadecyldimethylbetaine (C_{18}DMB). The dilute to semidilute crossover concentration was found to be approximately 0.35% concentration by weight from both light scattering and viscosity data. The results from the dynamic light scattering data were significantly better described by a model with two decay times, rather than a single decay, cumulants model. The dynamic light scattering data were also fit to a Kohlrausch−Williams−Watts form, which is consistent with translational diffusion and internal modes. The light scattering, viscosity, and cryo-TEM data are all consistent with the existence of long rodlike micelles. The critical micellar concentration, cmc, was determined via surface tension measurements and found to be 5×10^{-6} M at 40 °C.

Introduction

The study of the properties of micelles in aqueous solutions has a rich history. In recent years there has been a great deal of experimental and theoretical interest in studying the growth of micelles under appropriate solution conditions from approximately spherical minimum micelles to rodlike spherocylinders.[1−20] One of the more common probes of this behavior has been static and dynamic light scattering.[1−3,7,12,15−23] These experiments have been interpreted to indicate that the resulting micelles are flexible objects[4,16,25−30] and that at very modest concentrations, of order a few weight percent, these micelles may entangle and form a semidilute solution.[16,19,25] This micellar growth has been observed and explained in a wide variety of surfactant types including ionic,[1−3,15,16,18] nonionic,[17,19,20,22] and zwitterionic surfactants.[23,30−33]

The latter two families of surfactants are of interest because they are in some ways similar to proteins, and they presumably have somewhat simpler electrostatic interactions than micelles formed from ionic surfactants. Zwitterionic surfactants, which are electrically neutral compounds in which charged subgroups are separated by intervening atoms, show behavior that is different from that observed in nonionic surfactants. For example, solutions of the zwitterionic surfactant C_8-lecithin exhibits an upper consolute point,[31−33] while the nonionic ethoxylated alcohols (C_iE_j, where i is the number of carbons in the hydrophobic alkyl chain and j is the number of ethylene oxide groups in the headgroup) form solutions that exhibit a lower consolute point.[34] This difference is in part due to hydrogen bonding in these nonionic surfactants. Interestingly, the location of the cloud temperature in both these systems is affected by ionic additives.[21,23,31−33]

Another interesting example of zwitterionic surfactants are the *n*-alkyldimethylbetaines. These surfactants are interesting because, even in pure water, sufficiently long hydrocarbon chain length members of this family form long rodlike micelles, whose observed behavior is remarkably temperature independent.[35] Furthermore, the work of Fendler and Benton[36] shows that there are no phase transitions above the Krafft temperature, and the work of Bhatia and Qutubuddin[23] (and the present work) shows that there is no temperature dependence in the dynamic light scattering behavior. Thus, these types of systems are good models for understanding the statistical mechanics and thermodynamics of micellar aggregation and interactions.

The present paper describes dynamic light scattering, surface tension, viscometric, and cryo-TEM studies of one member of this family, octadecyldimethylbetaine, $CH_3(CH_2)_{17}N^+(CH_3)_2$-$CH_2COO^-$, or C_{18}DMB. This surfactant has a very low cmc—our measurements at 40 °C indicate that it is 5×10^{-6} M—and has a Krafft temperature of approximately 32 °C.[36] The effects of surfactant concentration and the lack of temperature dependence in both the specific viscosity and the apparent hydrodynamic radius will be presented. It will be shown that the temperature dependence of the diffucion coefficient can be explained in terms of its dependence on the absolute temperature and the shear viscosity.

Experimental Methods

Materials. The surfactant C_{18}DMB was synthesized at the British Petroleum Laboratory in Warrensville, OH, supplied to us by Dr. Eleanor Fendler and was used without further purification. The water used was first filtered and then deionized through a Millipore Milli-RO and a Milli-Q purification/filtration unit, for a final resistivity of 18 MΩ·cm.

Sample Preparation. Ten different concentrations were studied: 0.05, 0.075, 0.1, 0.15, 0.2, 0.5, 0.75, 1, 1.5, and 2 wt % concentration of surfactant in water. Light scattering quality round-bottom test tubes were carefully inspected for optical defects and scratches and then were cleaned and polished. The samples were prepared directly in the light scattering cells by the following method. First, 4 mL of purified water, further filtered by passing through an Anatop 0.22 μm filter, was added to the cell. Second, the appropriate mass of surfactant, measured to within 0.00005 g, was added to the cell. Third, to ensure that the surfactant had properly mixed, the resulting inhomogeneous solution was heated to 50 °C, for a minimum of 24 h.

[†] Also Department of Physics, Case Western Reserve University, Cleveland, OH 44106.

[‡] Present address: John Marshall Law School, Cleveland, OH.

* To whom correspondence should be addressed. E-mail: Fisch@JCVAXA.jcu.edu.

S1089-5647(98)01939-7 CCC: $15.00
Published on Web 08/01/1998

The homogeneity of the samples was further ensured by vortex mixing the heated sample at random intervals. The resulting samples were of good light scattering quality. Nevertheless, just before light scattering measurements were made, the samples were centrifuged at 5500 rpm and 40 °C for 30−45 min to further remove any residual dust from the sample. The resulting samples are very stable; measurements made more than 15 months apart are in close agreement.

Experimental Apparatus. The light scattering studies were conducted using a Malvern 4700 light scattering apparatus, with a Lexel model 95 laser operating at a wavelength, $\lambda = 514.5$ nm. Dynamic light scattering measurements were performed at three scattering angles: 60, 90, and 120°. At each angle and concentration four separate temperatures were studied: 35, 40, 45, and 50 °C. For each temperature, angle, and concentration studied, 50 30 s correlation runs were made.

The viscosity measurements were performed using a Brookfield DV-III cone and plate type viscometer. Viscosity measurements were made at each sample concentration and over the same temperature range as the light scattering measurements. The viscosity measurements were performed in two ways for all temperatures and concentrations. First, the shear rate was increased in discrete steps and the resulting shear strain measured. This established a shear rate operating range. Subsequent measurements were made at the same constant shear rate as a function of time. This allowed the observation of the time-dependent shearing qualities of the sample.

The surface tension was measured using a Fisher Scientific Autotensiomat du Nouy ring tensiometer. The reported values are apparent surface tensions uncorrected for the size of the ring or its diameter. The same water and batch of C_{18}DMB were used for these measurements as the light scattering and viscosity measurements. These measurements were performed at 40 ± 0.05 °C by serially diluting a sample of concentration 0.05% by factors of 2 until the surface tension approached that of pure water. Intermediate points between those obtained from this initial set of measurements were obtained by serially diluting a sample with a different initial concentration. At each concentration the apparent surface tension measurement was performed 2−4 times and then averaged.

The cryo-TEM samples were prepared by freezing 0.25, 0.5, and 1 wt % concentration samples in jets of liquid propane. The vitrified samples were transferred to a freeze fracture apparatus, fractures, and the water sublimated. The fractured surfaces were replicated by evaporation of platinum at an angle of 45° to the surface by a film of carbon. The replicas were washed and collected on 600 mesh electron microscope grids and examined using a JEOL 100C scanning transmission electron microscope in the conventional transmission mode at an electron energy of 80 keV. Further details are available elsewhere.[37]

Analysis

Dynamic Light Scattering. The data collected from the dynamic light scattering experiments were analyzed in several different ways. The first step was always to eliminate any correlation run that was of low quality on the basis of the following two criteria. First, any correlation runs in which the last delayed correlation channel and the calculated infinite time decay "far point" did not agree to within 0.5% were eliminated. Second, the remaining runs were graphed and visually inspected to see whether any runs lay substantially above the others; these runs presumably contain excessive noise or dust and were therefore eliminated. The number of runs kept was concentration-dependent. Generally between 20 and 50 of the 50 runs collected were kept. The lower number typically corresponded to dilute samples and a small scattering angle.

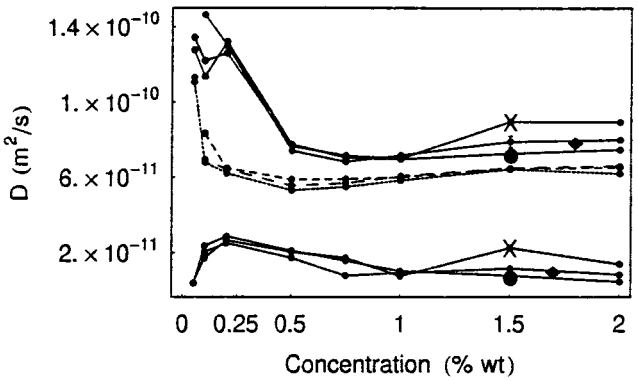

Figure 1. Diffusion coefficients at 40 °C for the biexponential and cumulant fits as a function of concentration for the three angles studied. The middle, dashed set is from the cumulants fit; the top and bottom sets are from the biexponential set. Angles are marked as follows: (◆) 60°, (×) 90°, (●) 120°. A typical error bar is shown.

The data were then fit to a number of models. First, the data were fit to a cumulants model using two different fit programs: the standard analysis which is in Malvern's automeasure program and a program that includes covariant noise.[38] The results from both of these programs are in close agreement. The effective mean hydrodynamic radius, $\langle R_h \rangle$, which measures average size in the dilute region, void size in the semidilute region, and lacks meaning around the crossover region, exhibited no systematic trends with temperature, T. The mean diffusion coefficient determined from the cumulants fit at 40 °C did vary strongly with concentration, as shown in Figure 1; starting from a maximum of 11×10^{-11} m^2/s at low concentrations, it reached a minimum at 0.5% concentration and slowly rose to a value of 6.5×10^{-11} m^2/s at 2.0% concentration. Significantly, the χ^2's and residuals of fits of the data to the cumulants form were uniformly very poor. Furthermore, the polydispersity parameters were ≥0.3. Together, these two observations strongly suggest that the population of decay times of the light scattered by the solution is either not unimodal or very polydisperse. To test the hypothesis of bimodal decay times, the data were fit to a series of multiexponential models of the form

$$G(\tau) = \sum_i^m (a_i e^{-\Gamma_i \tau})^2 \quad \text{and} \quad G(\tau) = (\sum_i^n a_i e^{-\Gamma_i \tau + c_i \tau^2})^2$$

where m and n were varied from 2 to 4 and 2 to 3, respectively, and a_i, Γ_i, and c_i are adjustable parameters corresponding to the amplitude, inverse decay time, and second cumulant, respectively. These fits, adjusted for degrees of freedom, were significantly better than the cumulant model fits.[38] It was found that the data could be adequately explained in terms of two distinct populations of decay times. The two decay times, Γ_i, that were obtained were separated by a factor of 8−20. The diffusion coefficients, defined through $D_i = \Gamma_i/q^2$, where q is the scattering vector, $q = (4\pi n/\lambda) \sin(\theta/2)$, n is the index of refraction of the solution, and λ is the vacuum wavelength of the incident laser and θ the scattering angle, and the percent fractions, a_i, exhibited very little q dependence and essentially no temperature dependence beyond that expected for constant size objects. There is, however, significant concentration dependencies to all three of these quantities.

The concentration dependence of the diffusion coefficient determined using cumulants and the two diffusion coefficients

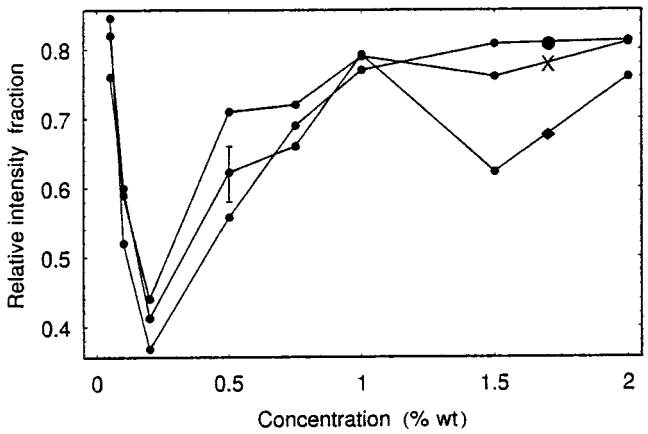

Figure 2. Relative intensity fraction of the larger coefficients from the biexponential fit as a function of concentration.. Angles are marked as follows: (◆) 60°, (×) 90°, (●) 120°. A typical error bar is shown.

that describe the bimodal distribution, determined at 40 °C and at scattering angles of 60, 90, and 120°, is shown in Figure 1. Because our data indicate that, except at the lower concentrations studied, the system is in the crossover and semidilute solution regime, these characteristic data for both the small and large coefficients represent that obtained by averaging the nearly temperature independent $\langle R_h \rangle$. The larger diffusion coefficient obtained a minimum value at a concentration of 0.2%, rose to a maximum between concentrations of 0.5% and 1% and then leveled off. The smaller diffusion coefficient obtained a maximum value of 3.5×10^{-11} m^2/s at a concentration between 0.75% and 1%, with generally constant behavior elsewhere. This maximum value was roughly twice the values observed at higher and lower concentrations. The extracted diffusion coefficients exhibited a small angular dependence, its value shifting upward in concentration with increasing angle.

The two populations did not scatter equally. The relative intensity, or the percent fraction of the total intensity that was attributed to the larger diffusion coefficient population, is shown as a function of concentration and scattering angle in Figure 2. At low concentrations this coefficient is roughly 80% of the total scattered intensity. Upon increasing concentration it dips to a minimum that averages 40% at a concentration of 0.2% and then rises back to 80% as the concentration further increases. Interestingly, the minimum in the large diffusion coefficient intensity fraction corresponds to the maximum value in both large and small diffusion coefficients. In light of the errors involved in the fitting, the intensity fraction is scattering angle independent. Since the sum of the two intensity fractions is 1, the relative intensity fraction for the small diffusion coefficient population is one minus the data in Figure 2.

As noted above, the cumulants fitting procedure is more useful in the dilute regime than in the semidilute regime, where there are a number of relaxation processes. In this situation the cumulants model yields a diffusion coefficient that is an average weighed by the various relaxation processes. Another approach to analyzing dynamic light scattering data in the semidilute regime has recently been presented by Galinsky and Burchard.[39−41] This consists of approximating each relaxation component by a stretch exponential or Kohlrausch−Williams−Watts (KWW) function. In this model the intensity autocorrelation function is given by

$$G(\tau) = [\sum_i a_i \exp(-t/b_i)^{\beta_i}]^2$$

with the constraints that $\sum_i a_i = 1$ and $0 \leq \beta \leq 1$. In this

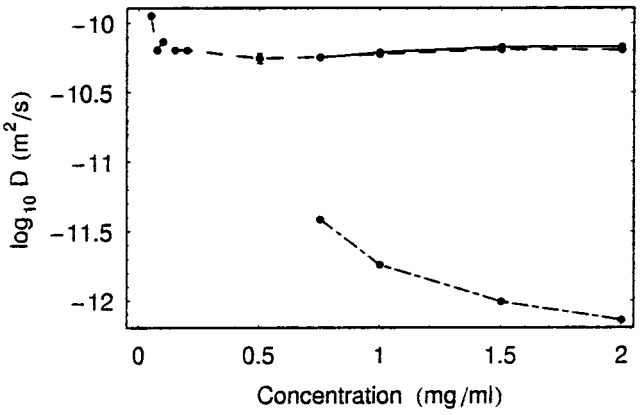

Figure 3. Diffusion coefficients determined from the cumulants fit (− −) and the two-population KWW fits (— and - − -). The error in the data is approximately the size of the data points.

expression the a_i are the weights (or amplitudes) of the ith relaxation process, and b_i and β_i characterize the ith mean relaxation time, $\langle \tau_i \rangle$, which is given by

$$\langle \tau_i \rangle = \frac{b_i}{\beta_i} \Gamma\left(\frac{1}{\beta_i}\right)$$

where $\Gamma(x)$ is the gamma function. The parameter β is a measure of the width of the distribution. $\beta = 1$ corresponds to a single exponential, and hence a very narrow distribution, while a smaller β corresponds to a broader distribution.

We found the use of a two-population KWW model leads to excellent fits to the experimental data. These fits are statistically indistinguishable from the two-exponential fits discussed above. The results are interesting. For concentrations greater than 0.5% the behavior is systematic. There are two distinct modes. The first mode has decay times proportional to q^{-2} and β near 1. The second mode has β near 0.5 and displays a stronger angular dependence than q^{-2}. This behavior along with the cumulants fits is shown in Figure 3, which is a graph of the calculated diffusion coefficient at a temperature of 40 °C and a scattering angle of 90° for the strongly angular dependent mode as a function of concentration. Finally, the two-population KWW model is significantly more physical than the cumulants model for concentrations greater than 0.5%. However, from the standpoint of both the χ^2 and F tests the KWW model fits are not significantly superior. In this higher concentration region the cumulant fits obtain polydispersities between 0.5 and 0.6.

The physical interpretation of these two modes appears to be straightforward. The fast mode, corresponding to the slowly increasing diffusion coefficient with concentration, obtains a value $\beta = 0.92 \pm 0.02$ and the same diffusion coefficient independent of scattering angle. This means that this mode corresponds to the diffusion of an essentially monodisperse object. This is most likely the cooperative diffusion mode. One potential difficulty with this interpretation is that one would expect D_{coop}, the cooperative diffusion coefficient, to exhibit a fairly strong power law dependence with concentration of the form $D_{coop} \propto c^x$, with the value of x between 0.5 and 1. In the semidilute regime $x = 0.75$ is predicted,[42] while typical experimental values appear to be between 0.5 and 1.[43] The current experiment yields a value $x = 0.19 \pm 0.04$. This small value may be due to the relative poorness of the solvent. Our laboratory was unable to obtain well-mixed samples with concentrations above 2%. Last, there is little concentration or angular dependence to the weight, A_f, of this mode. It has an

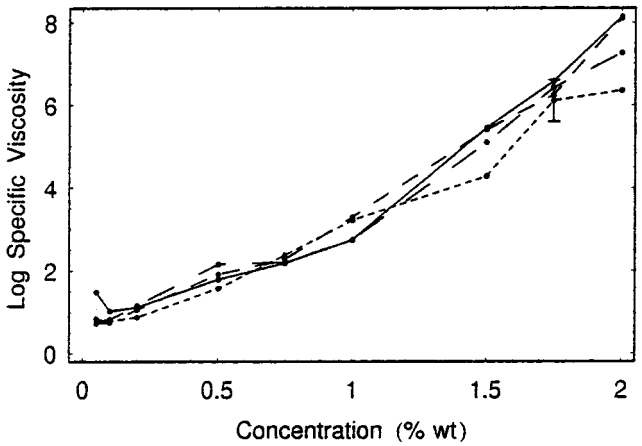

Figure 4. The log of the specific viscosity measured versus concentration. These data are very nearly linear, which implies an exponential concentration dependence. The temperatures in °C are (---) 35, (---) 40, (− −) 45, and (—) 50. A typical error bar is shown.

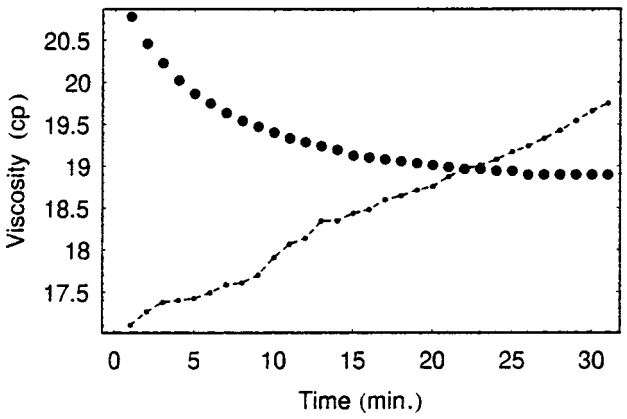

Figure 5. Two typical viscosity runs are shown as a function of time. These runs, performed at constant shear and similar temperatures, clearly show dissimilar trends: one shear thinning and one shear thickening. The error in the data is approximately the size of the data points.

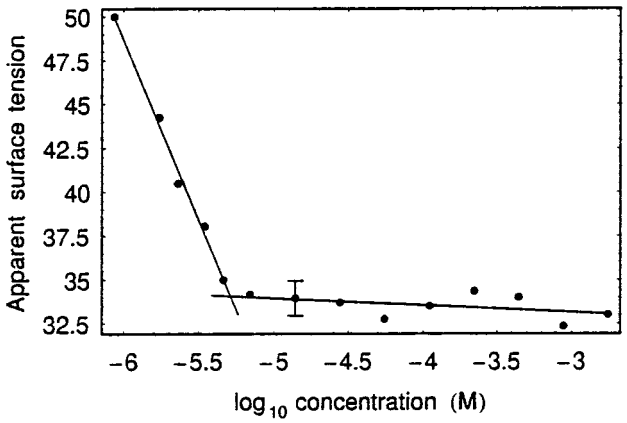

Figure 6. Apparent surface tension vs log of the molar concentration of C_{18}DMB at 40 °C. The break in the curve, indicating the cmc, is approximately 5×10^{-6} M. A typical error bar is shown.

average weight of 80 ± 2% of the total weight throughout the whole semidilute regime.

The second mode has a stronger and more irregular scattering vector dependence. This mode obtains $\beta = 0.5 \pm 0.1$ independent of concentration. The interpretation of this mode as polydisperse aggregates diffusing in the semidilute network is not likely since there is no systematic angular variation in the calculated diffusion coefficient. More likely, this should be expressed as a broad range of decay times which correspond to internal modes of the transient clusters that form in the semidilute solution. Although this mode is commonly observed, we know of no unequivacable interpretation of its physical significance.[43,44]

Viscosity. The solutions exhibited non-Newtonian behavior for concentrations greater than approximately 0.5%. However, the viscosity of these solutions, measured long after the uniform shearing of the sample began, was temperature-independent. We observed both time-dependent shear thinning and shear thickening as indicated in Figure 4. While it appears that there was a change from shear thinning to shear thickening near 40 °C, there are enough exceptions to this behavior that this should not be taken as a strong rule. The relative viscosity determined from the long time behavior increased exponentially with concentration, starting with a value close to that of water for the lowest concentration and rapidly increasing to a final value of approximately 1700 cP at a concentration of 2.0%. A graph of the log of the specific viscosity, $\eta_i = (\eta_{solution} - \eta_{water})/\eta_{water}$, where η is the shear viscosity in poise, versus concentration is shown in Figure 5. These data are well reproduced by the equation

$$(\eta_{solution} - \eta_{water})/\eta_{water} = 0.1e^{490x}$$

where x is the weight concentration of surfactant. This empirical fit is substantially better than fits to the form $\eta_i \propto x^n$, where n is an adjustable parameter.[45]

Surface Tension. The concentration region where surfactant molecules change from acting as essentially independent molecules on the surface to forming micelles is called the critical micellar concentration, or cmc. The apparent surface tension was measured at both 25 and 40 °C. Since 25 °C is below the Krafft temperature, it will not be discussed except to state that the measured cmc was 5×10^{-5} M. The surface tension as a function of concentration at 40 °C is shown in Figure 6. This figure indicates that there is no minimum in the surface tension as surface-active impurities would cause. Extrapolation of linear curves from above and below the break point in the curve yields a cmc of 5×10^{-6} M. This is consistent with what one would expect based on the cmc vs chain length data of Fendler et al.[36] provided one assumes that the cmc is essentially temperature independent above the Krafft temperature.

Cryo-TEM. The cryo-TEM data are consistent with the existence of rodlike micelles and semidilute solution behavior at higher concentrations. The results, as shown in Figure 7, indicate that the molecules form rodlike structures and that the rods form an entangled network. This type of structure was very evident throughout both the 0.5 and 1% samples that were studied. The 0.25% sample that was examined had very little structure indicative of an entangled network. Instead, it consisted primarily of quasi-random rodlike or elliptical structures.

Discussion

The rapid increase in viscosity with concentration as well as the cryo-TEM photographs indicates that the micelles are large rodlike or wormlike micelles.[1,2,16,24,25,30] This conclusion is consistent with the findings of Bhatia and Qutubuddin,[23] who report long, semiflexible micelles. However, our data extend their findings in several ways. First, in light of the large polydispersity of the cumulants fits the two diffusion coefficient model for the correlation function provides a more sound

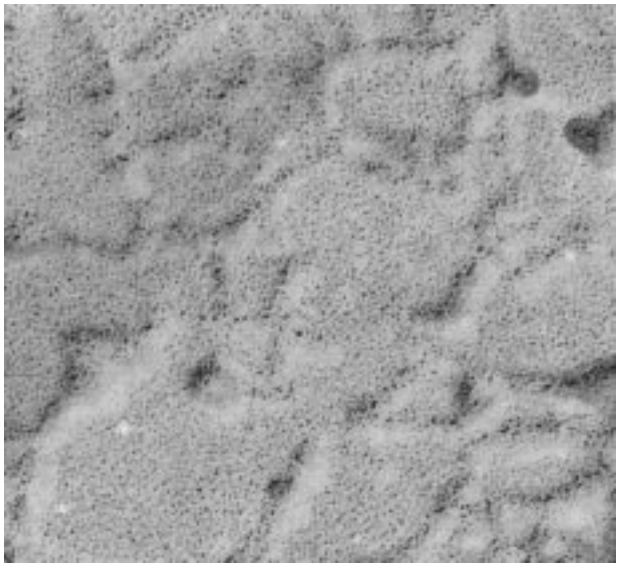

Figure 7. Cryo-TEM photograph of 0.5% C_{18}DMB sample. Magnification = 218 000. The small black particles are the result of sample preparation. The random network of wormlike structures is believed to be the micelles.

physical interpretation of the data than a monomodal distribution, especially at higher concentrations. The simple one-dimensional growth model of micelles[2,3,9,10] assumes that the solutions are dilute and that the mean aggregation number is proportional to the square root of the mole fraction of surfactant above the cmc. While the latter may be true for very low concentrations, in the present study the more easily studied concentration regime is the semidilute regime. A simple criteria for the crossover concentration, c^*, from dilute to semidilute solution is $c^* = 1/[\eta]$, where $[\eta]$ is the intrinsic viscosity.[45] When this model is applied to the present viscosity data, the resulting crossover concentration is predicted to occur near a concentration of 0.35%. This indicates that most of the accessible concentration region from dilute to maximum concentration has been studied. Furthermore, there is no concentration in the present study where intermicellar interactions are negligible. As seen in Figures 1−3, in the region near c^* there are significant variations in the static and dynamic light scattering data. Generally, a minimum in the diffusion coefficient occurs at the crossover concentration.[19,25] Such a minimum in the diffusion coefficient as determined by the cumulants method, and for the larger diffusion coefficient of the bimodal fits, occurs near but slightly above this concentration. These minima support the conclusion that the crossover concentration occurs at a concentration near 0.35−0.50%. However, the support of this view is not total as there is a maximum in the smaller diffusion coefficient, obtained from the biexponential model, at concentrations slightly below this crossover concentration. Furthermore, the intensity fraction scattered by this smaller diffusion coefficient population is a larger fraction of the total intensity at the concentration at which the maximum is obtained.

We believe that the apparent bimodal distribution of decay times in the data are real and not artifacts. First, the data are reproducible: three identical separate dynamic and static light scattering and viscosity measurements were made over a period of 2 years. Also, samples that were reexamined gave identical results, to within the errors, even when studied up to 9 months apart. The sample obtained from Fendler appears to be fairly pure. A purity assay of the sample indicated that it was >95% pure, with no ionic contaminants or residual acids from the synthesis process. Second, surface tension measurements are also an indicator of contaminants. Any surface-active contaminants will cause a minimum in the surface tension vs concentration curve near the cmc. No such minimum was seen in our measurements.

Conclusion

We have examined the zwitterionic surfactant C_{18}DMB in water using dynamic light scattering, surface tension, cryo-TEM, and viscosity measurements. Our results concur with previously reported investigations by Bhatia and Qudubuddin,[23] in that we find little or no temperature dependence in the viscosity or apparent hydrodynamic radius across the concentration range studied, and all of the data results indicate that this system is composed of large rodlike micelles or similarly shaped objects. However, the results differ from theirs in several ways. First, the correlation functions are better fit to a two-decay time model rather than a cumulants model. In the semidilute solution regime the second decay is consistent with internal modes. Second, all of the measurements point to a dilute to semidilute crossover in the 0.2−0.5% concentration range, with the best estimate of c^* being 0.35%. Third, although the data indicate that the solution is composed of long rodlike objects, the polydispersity parameters obtained from cumulant fits are large (0.3−0.7, depending on the number of channels fit, the inclusion of background terms, and other parameters) for polydisperse self-assembled rods. Even in the dilute solution regime a two-exponential, or two-population, model for the intensity correlation function is better. One would expect[1−3,9,10] a unimodal distribution and in light of the rather modest growth a smaller polydispersity. Thus, a self-consistent model that describes the present data even in the dilute solution regieme is lacking.

The relative simplicity of the thermodynamics of this system, as it is zwitterionic and the growth even in the dilute solution regime is temperature-independent, makes this a more ideal system for theoretical models than many other families of surfactants. We hope that these results might motivate such work.

Acknowledgment. This work was supported by Advanced Liquid Crystal Institute for Optical Materials (ALCOM) Grant DMR-8920147 and NSF Grant DMR-9321924. Mr. Joseph Polak of Case Western Reserve University assisted us with the cryo-TEM experiments. We also wish to thank the referee for helpful and stimulating comments on an earlier version of this manuscript.

References and Notes

(1) Young, C. Y.; Missel, P. J.; Mazer, N. A.; Benedek, G. B.; Carey, M. C. *J. Phys. Chem.* **1978**, *82*, 1375.
(2) Missel, P. J.; Mazer, N. A.; Benedek. G. B.; Young, C. Y.; Carey, M. C. *J. Phys. Chem.* **1980**, *84*, 1044.
(3) Missel, P. J.; Mazer, N. A.; Benedek. G. B.; Carey, M. C. *J. Phys. Chem.* **1983**, *87*, 1264.
(4) Porte, G.; Appell, J.; Poggi, Y. C. *J. Phys. Chem.* **1980**, *84*, 3105.
(5) Van De Sande, W.; Persoons, A. *J. Phys. Chem.* **1985**, *89*, 404.
(6) Imae, T.; Ikeda, S. *J. Phys. Chem.* **1986**, *90*, 5216.
(7) Briggs, J.; Nicolli, D. F.; Ciccolello, R. *Chem. Phys. Lett.* **1980**, *73*, 149.
(8) Tanford, C. *J. Phys. Chem.* **1974**, *78*, 2469.
(9) Israelachvilli, J. N.; Mitchell, D. J.; Ninham, B. W. *J. Chem. Soc., Faraday Trans. 2* **1976**, *72*, 1525.
(10) Mukerjee, P. *J. Phys. Chem.* **1972**, *76*, 565.
(11) Ikeda, S. *J. Phys. Chem.* **1984**, *88*, 2144.
(12) Porte, G. *J. Phys. Chem.* **1983**, *87*, 3541.
(13) Eriksson, J. C.; Ljunggren, S. *J. Chem. Soc., Faraday Trans. 2* **1985**, *81*, 1209.

(14) Nagarajan, R.; Shah, K. M.; Hammond, S. *Colloids Surf.* **1982**, *4*, 147.
(15) Missel, P. J.; Mazer, N. A.; Carey, M. C.; Benedek. G. B. *J. Phys. Chem.* **1989**, *93*, 8366.
(16) Mishic, J. R.; Fisch, M. R. *J. Chem. Phys.* **1990**, *92*, 3222.
(17) Puvvada, S.; Blankschtein, D. *J. Chem. Phys.* **1990**, *92*, 3710.
(18) Fisch, M. R.; Benedek, G. B. *J. Chem. Phys.* **1986**, *85*, 553.
(19) Kole, T. M.; Richards, C. J.; Fisch, M. R. *J. Phys. Chem.* **1994**, *98*, 4949.
(20) Stephany, S. M.; Kole, T. M.; Fisch, M. R. *J. Phys. Chem.* **1994**, *98*, 11126.
(21) Douglas, C. B.; Kaler, E. W. *Langmuir* **1991**, *7*, 1097.
(22) Wilcoxon, J. P.; Kaler, E. W. *J. Chem. Phys.* **1987**, *86*, 4684. Wilcoxon, J. P.; Schaefer, D. W.; Kaler, E. W. *J. Chem. Phys.* **1990**, *90*, 1909.
(23) Bhatia, A.; Qutubbin, S. *Colloids Surf.* **1993**, *69*, 277.
(24) Imae, T.; Ikeda, S. *J. Phys. Chem.* **1985**, *90*, 5216. Imae, T.; Ikeda, S. *Colloid Polym. Sci.* **1987**, *265*, 1090.
(25) Cates, M. E.; Candau, S. J. *J. Phys.: Condens. Matter* **1990**, *2*, 6869 and references therein.
(26) Candau, S. J.; Hirsh, E.; Zana, R. In *Physics of Complex and Supermolecular Fluids;* Safran, S. A., Clark, N. A., Eds.; Wiley: New York, 1987; p 569.
(27) Candau, S. J.; Hirsch, E. Zana, R.; Delsanti, M. *Langmuir* **1989,** *5*, 1225.
(28) Kato, T.; Anzai, S.; Seimiya, T. *J. Phys. Chem.* **1990**, *94*, 7255.
(29) Schurtenberger, P.; Magid, L. J.; Penfold, J.; Heenan, R. *Langmuir* **1990**, *6*, 1800.
(30) Mazer, N. A. In *Dynamic Light Scattering*; Pecora, R., Ed.; Plenum Press: New York, 1985.
(31) See, for example: Thurston, G. M. Thesis, MIT, 1986, or Blankschtein, D.; Huang, Y.; Thurston, G. M.; Benedak, G. B. *Langmuir* **1991**, *7*, 897.
(32) Tausk, R. J. M.; Oudshoorn, C.; Overbeek, J. Th. G. *Biophys. Chem.* **1974**, *2*, 53.
(33) Tausk, R. J. M.; Overbeek, J. Th. G. *Biophys. Chem.* **1974**, *2*, 175.
(34) There is a large literature in this area. See, for instance, refs 21 and 22 above and Corti, M.; Degiorgio, V. *J. Phys. Chem.* **1981**, *85*, 14425; **1984**, *88*, 309.
(35) Swarbrick, J.; Daruwala, J. *J. Phys. Chem.* **1970**, *74*, 1293.
(36) Fendler, E. J.; Benton, W. J., personal communication.
(37) See, for example: Zasadzinski, J. A. N.; Chu, A.; Prud'homme, R. K. *Macromolecules* **1986**, *19*, 2960.
(38) Harrison, D.; Fisch, M. R. *Langmuir* **1996**, *12*, 6691.
(39) Galinsky, G.; Burchard, W. *Macromolecules* **1995,** *28*, 2363.
(40) Galinsky, G.; Burchard, W. *Macromolecules* **1996,** *29*, 1498.
(41) Galinsky, G.; Burchard, W. *Macromolecules* **1997,** *308*, 4445.
(42) See for instance: Doi, M. *Introduction to Polymer Physics*; Oxford: New York, 1996. Doi, M.; Edwards, S. F. *The Theory of Polymer Dynamics*; Oxford: New York, 1986.
(43) (30) Schaefer, D. W.; Han, C. C. In *Dynamic Light Scattering*; Pecora, R., Ed.; Plenum Press: New York, 1985.
(44) Brown, W., Ed. *Dynamic Light Scattering*; Oxford: New York, 1993.
(45) For rodlike micelles one would expect $\eta_i \propto x^n$. See: Porte, G. In *Micelles, Membranes, Microemulsions, and Monolayers*; Gelbart, W. M., Ben-Shaul, A., Roux, D., Eds.; Springer: New York, 1994; Chapter 2. The optimal value of the exponent *n* for the present data is 9. However, this fit is substantially worse than the exponential fit.